



# A Predictive Model for Pullout Bearing Resistance of Geogrids Embedded in a Granular Soil

G. Cardile<sup>(✉)</sup>, M. Pisano, and N. Moraci

Department of Civil Engineering, Energy,  
Environment and Materials (DICEAM),  
“Mediterranea” University of Reggio Calabria, Via Graziella,  
89122 Reggio Calabria, Italy  
giuseppe.cardile@unirc.it

**Abstract.** Currently, Geosynthetic-Reinforced Soil (GRS) structures represent one of the most sustainable solutions capable to improve the protection of the territory, guaranteeing high performance (especially in seismic field) with construction costs that are lower than those required for the more traditional Civil and Environmental engineering works. To design such types of structures the knowledge of soil-geosynthetic interface parameters is necessary, and their prediction is very complex due to the elementary interaction mechanisms affecting the pullout resistance of geogrids embedded in soils that are mainly the skin friction between soil and the reinforcement’s solid surface, and the bearing resistance developing on transverse elements. When the spacing between the geogrid’s transverse elements is below a threshold value, the interference mechanism develops and it can affect the bearing resistance, as the passive surfaces cannot be entirely mobilised on bearing members. In order to model the peak pullout resistance of extruded geogrids embedded in a compacted granular soil, the paper deals with a new experimental validation of a theoretical method taking into account the interference mechanism.

**Keywords:** Geosynthetics · Theoretical model · Pullout bearing resistance · Interaction mechanisms · Interference

## 1 Introduction

In the last decades, the use of geosynthetics to design geotechnical and environmental engineering measures allows improving their behaviour towards both the ultimate and the serviceability limit state, concurrently reducing construction costs and the environmental impact. Therefore, design with geosynthetics provides engineering solutions that better satisfy the principal sustainability criteria for construction in an era where the environmental impact reduction has become a requirement.

With regard to geosynthetic reinforced soil structures, it is important to calculate the soil-geosynthetic interaction parameters conveniently (Carbone et al. 2015; Cardile et al. 2016a; 2019; Ezzein and Bathurst 2014; Ferreira and Zornberg 2015; Moraci and Cardile 2008, 2009, 2012; Moraci et al. 2017; Pavanello et al. 2018a, b; Zhou et al.

2012). The prediction of the aforementioned parameters can be very complex for soil-geogrid interfaces due to the open structure of this type of geosynthetic. In fact, with regard to the pullout resistance two elementary interaction mechanisms mainly affect the results, i.e. the skin friction between soil and the solid surface of reinforcement, and the bearing resistance developing on transverse elements. The mobilisation of these interaction mechanisms depends on different factors, such as geometrical and mechanical characteristics of the polymeric reinforcement, the physical properties and the mechanical characteristics of the soil in contact, the effective stress state acting on the interface, the loading conditions. According to several researches (Bergado et al. 1993; Calvarano et al. 2014; Dyer 1985; Jewell 1996; Milligan et al. 1990; Palmeira 2009; Palmeira and Milligan 1989), the bearing resistance can be affected by both the scale effect and the interference phenomenon. In the paper, a previous model developed by Cardile et al. (2017a) to determine the peak pullout resistance of extruded geogrids embedded in a compacted granular soil taking into account the interference phenomenon (with the introduction of a reduction factor,  $C_{zb}$ ) has been validated by means of additional pullout tests. Specifically, new reduction factors have been calculated by using a purely experimental procedure, verifying the good prediction of the model in a range of values not investigated previously.

## 2 Pullout Resistance: Theoretical Prediction

According to (Jewell 1990), the pullout resistance of soil-geogrid interfaces can be obtained as the sum of two contributions, which are assumed to be not dependent on each other to simplify the problem:

$$P_R = P_{RS} + P_{RB} \tag{1}$$

In the Eq. (1)  $P_{RS}$  and  $P_{RB}$  are the skin friction and the bearing components of pullout resistance, respectively.

Cardile et al. (2017a) proposed a theoretical method taking into account the interference phenomenon, which occurs when the ratio of the spacing  $S$  between the geogrid bearing members to the thickness of the transverse bars  $B_{eq}$  is below a threshold value. The method, which works well for soil-geogrid interfaces where the scale effect is negligible (ratio of  $B_{eq}$  to the soil average grain size  $D_{50}$  exceeding a threshold value), provides the peak pullout resistance of extruded geogrids embedded in a compacted granular soil as follows:

$$P_R = 2 \cdot C_{\alpha S} \cdot \alpha_S \cdot L_R \cdot \sigma'_n \cdot \tan \delta + C_{zb} \cdot n_t \cdot n_{tb} \cdot A_b \cdot \sigma'_b \tag{2}$$

$$C_{zb} = \begin{cases} \alpha \cdot \frac{S}{B_{eq}} & \text{for } \frac{S}{B_{eq}} \leq 50 \\ 1 & \text{for } \frac{S}{B_{eq}} > 50 \end{cases} \tag{3}$$

where  $C_{\alpha_S}$  is a reduction coefficient to take into account the geogrid's area in which skin friction actually develops;  $\alpha_S$  is the fraction of geogrid's surface area that is solid;  $L_R$  is the length of geogrid;  $\sigma'_n$  is the vertical effective stress acting on the interface;  $\delta$  is the skin friction angle between soil and the geogrid;  $n_t$  is the number of geogrid's bearing members;  $n_{tb}$  is the number of nodes in a transverse element;  $A_b$  is the area of each transverse bar's element, which includes the single node and the bar portion between two nodes, where the bearing resistance can be mobilised;  $\sigma'_b$  is the bearing stress;  $\alpha = 0.02$  is a constant coefficient obtained by linear regression on pullout tests; and  $S/B_{eq}$  is the parameter which allows finding out whether or not the interference phenomenon can reduce the pullout resistance.

In Cardile et al. (2017a) model, the reduction coefficient  $C_{\alpha_b}$  was determined by using both experimental results of pullout tests ( $P_R^{exp}$ ) and the theoretical expression for the skin friction component ( $P_{RS}^{theor}$ ) provided by Moraci and Giofrè (2006):

$$C_{\alpha_b} = \frac{P_R^{exp} - P_{RS}^{theor}}{n_t \cdot n_{tb} \cdot A_b \cdot \sigma'_b} \quad (4)$$

In the Eq. (4), the skin friction angle  $\delta$  is assumed equal to  $1/3 \phi'$  (Fannin and Raju 1993; Moraci and Giofrè 2006; Raju 1995). For  $\phi'$  an average value between the peak shear strength angle and the one at constant volume is used in order to take into account the soil dilatancy and the reinforcement extensibility effects.

The bearing stress is evaluated by means of the Eq. (5) proposed by Matsui et al. (1996), which is based on Prandtl's local failure mechanism:

$$\frac{\sigma'_b}{\sigma'_n} = e^{\pi \tan \phi'} \cdot \tan \left( \frac{\pi}{4} + \frac{\phi'}{2} \right) \cdot \left[ \cos \left( \frac{\pi}{4} - \frac{\phi'}{2} \right) + (1 - \sin \phi') \cdot \sin \left( \frac{\pi}{4} - \frac{\phi'}{2} \right) \right] \quad (5)$$

In this case, for the soil shear strength angle  $\phi'$  the peak value corresponding to the different vertical effective stresses is used.

In the current research, the model has been validated verifying its good prediction in a new range of  $S/B_{eq}$  values. New reduction coefficients  $C_{\alpha_b}$  have been calculated by means of a purely experimental procedure, which uses the results of pullout tests carried out on both an HDPE transverse bar whose results are affected by the interference phenomenon ( $S/B_{eq} = 25.21$ ) and a stainless steel transverse bar for which the interference phenomenon is negligible ( $S/B_{eq} = 74.4$ ), having comparable  $B_{eq}$  values:

$$C_{\alpha_b} = \frac{\sigma'_{Rb} (HDPE \text{ bar})}{\sigma'_{Rb} (\text{steel bar})} \quad (6)$$

where  $\sigma'_{Rb} (HDPE \text{ bar})$  and  $\sigma'_{Rb} (\text{steel bar})$  are the peak bearing stress of the HDPE bar and the steel bar respectively.

### 3 Experimental Program

The experimentation was performed carrying out pullout tests under a constant rate of displacement (CRD = 1 mm per min) until the specimen’s pullout or the maximum displacement that the apparatus allows (100 mm) was reached.

The soil used in the research was an uniform medium sand classified as A-3 (UNI EN ISO 14688-1, 2018), with uniformity coefficient and average grain size equal to  $U = 1.96$  and  $D_{50} = 0.32$  mm respectively. The soil was compacted at a dry unit weight value equal to the 95% of the maximum dry unit weight obtained by Standard Proctor compaction tests ( $\gamma_{dmax} = 16.24$  kN/m<sup>3</sup> at an optimum water content  $w_{opt} = 13.5\%$ ). With regard to the mechanical behaviour, the soil peak shear-strength angles range from  $\phi'_p = 48^\circ$  at  $\sigma'_n = 10$  kPa to  $\phi'_p = 42^\circ$  at  $\sigma'_n = 100$  kPa, and the soil shear-strength angle at constant volume is equal to  $\phi'_{cv} = 34^\circ$  (Moraci and Cardile 2008; Moraci et al. 2014).

Two vertical effective stresses ( $\sigma'_n = 10$  and 100 kPa) were investigated on different specimens in order to comprehend the bearing interaction mechanism influencing the pullout resistance. Specifically, the pullout tests were performed on:

- an HDPE uniaxial extruded geogrid (specimen with two transverse bars, one of which is attached to the clamp), whose mechanical behaviour (Table 1) was investigated by means of wide-width tensile tests at the same rate used in the pullout tests (Cardile et al. 2016b, 2017b);
- the clamp in order to eliminate the soil-clamp friction by subtracting these results, at the same displacement value, from the previous pullout curves;
- the abovementioned HDPE uniaxial extruded geogrid where the transverse bar was removed (that is, specimen having only the longitudinal ribs);
- a stainless steel grid assembled ad hoc by means of five longitudinal ribs and a transverse bar both having a round cross-section ( $d = 2$  and 5 mm respectively).

**Table 1.** Wide-width tensile test results of the geogrid used in this research

$T_{max}$ ( $\epsilon' = 20\%/min$ ) [kN/m]	$\epsilon_{max}$ ( $\epsilon' = 20\%/min$ ) [kN/m]	$J_{sec2\%}$ ( $\epsilon' = 20\%/min$ ) [kN/m]	$T_{max}$ ( $\epsilon' = 0.2\%/min$ ) [kN/m]	$\epsilon_{max}$ ( $\epsilon' = 0.2\%/min$ ) [kN/m]	$J_{sec2\%}$ ( $\epsilon' = 0.2\%/min$ ) [kN/m]
Maximum tensile strength per unit width	Tensile strain for $T_{max}$ ( $\epsilon' = 20\%/min$ )	Secant tensile stiffness at 2% strain	Maximum tensile strength per unit width	Tensile strain for $T_{max}$ ( $\epsilon' = 0.2\%/min$ )	Secant tensile stiffness at 2% strain
159	12.2	2454	103.5	14.5	1525

## 4 Pullout Test Results

### 4.1 HDPE Geogrid

Figure 1a illustrates the pullout curves (pullout strength versus displacement of the first confined section of specimen) obtained for the soil-geogrid interface tested at two different vertical effective stresses ( $\sigma'_n = 10$  and 100 kPa). These curves have been used to calculate the trend in the bearing component  $P_B$  of the pullout strength (Fig. 1b) subtracting from them, at the same displacement value, those from tests carried out on specimen having only the longitudinal ribs. Results show a strain-softening trend due to the interference phenomenon, which entailed the decay in pullout resistance since the advancing of the clamp formed a disturbed region (softened region, Zhou et al. 2012), thus affecting the bearing resistance surface developing along the transverse bar. Moreover, peak values have been evaluated in order to quantify the contribution of the bearing component on the overall pullout strength: specifically, the peak bearing component  $P_{RB}$  represents the 72% of the peak pullout resistance  $P_R$ .

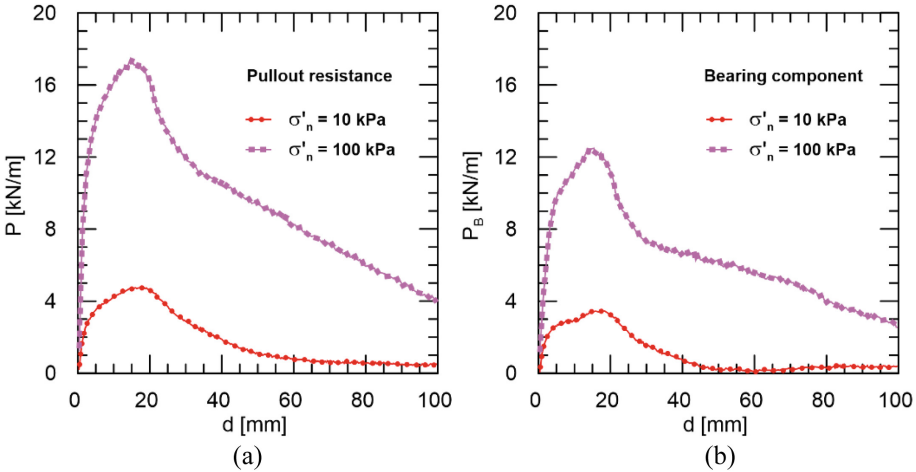


**Fig. 1.** Pullout strength (a) and bearing component (b) for varying the displacement of the first confined section of specimen, obtained for the soil-geogrid interface tested at  $\sigma'_n = 10$  kPa and 100 kPa

### 4.2 Steel Bar

In the following, to quantify the interference effect pullout tests at the same test condition were performed on interface made up of soil and a stainless steel transverse bar for which the interference phenomenon is negligible ( $S/B_{eq} = 74.4$ ). Figure 2 illustrates the trend in the bearing component  $P_B$  of the pullout strength for varying the displacement of the clamp, obtained for the soil-steel bar interface tested at two different vertical effective stresses ( $\sigma'_n = 10$  and 100 kPa). In this case the results show a strain-hardening behaviour since the distance between the clamp and the steel bar is large enough to allow maximising the development of the bearing resistance surface.

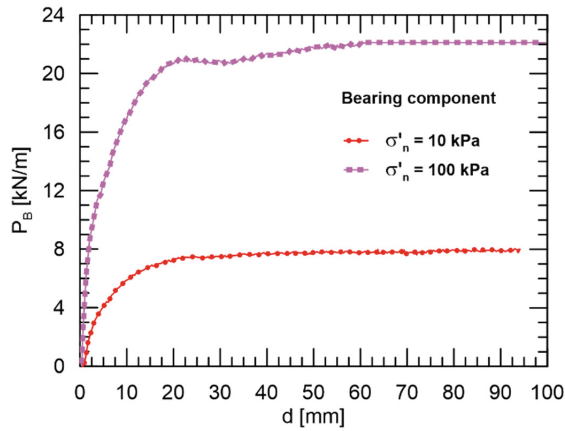


Fig. 2. Bearing component of the pullout strength for varying the displacement of the clamp, obtained for the soil-steel bar interface tested at  $\sigma'_n = 10$  kPa and 100 kPa

### 5 Model Validation

The validation of Cardile et al. (2017a) model has been performed by calculating the reduction coefficients according to Eq. (6). The obtained results have been plotted in Fig. 3 (square symbol), where it is possible to observe the model’s good prediction in a new range of  $S/B_{eq}$  values ( $S/B_{eq} = 25.21$ ). Specifically, the standard deviation of the experimental coefficient  $C_{\alpha b}$  in relation to the one obtained by Eq. (3) is equal to 0.01.

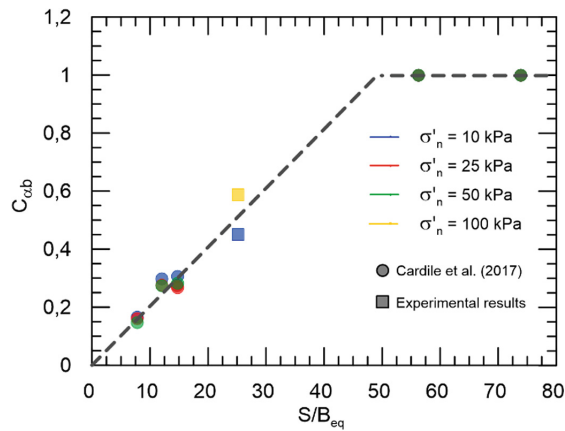


Fig. 3. Trend in the reduction coefficient  $C_{\alpha b}$  for varying the normalised spacing

## 6 Conclusions

The paper aims to validate by means of additional pullout tests a theoretical model, which predicts the pullout resistance of geogrids embedded in granular soils under pullout conditions, taking into account the interference effect that can reduce the bearing component developing on transverse elements when the spacing between the geogrid's transverse elements is below a threshold value.

New reduction factors have been calculated by using a purely experimental procedure, verifying the good prediction of the model in a range of values not investigated previously. The experimental results confirmed the good prediction of the model.

## References

- Bergado DT, Shivashankar R, Alfaro MC, Chai J-C, Balasubramaniam AS (1993) Interaction behaviour of steel grid reinforcements in a clayey sand. *Geotechnique* 43:589–603
- Calvarano LS, Giofrè D, Cardile G, Moraci N (2014) A stress transfer model to predict the pullout resistance of extruded geogrids embedded in compacted granular soils. In: 10th international conference on geosynthetics, ICG 2014, Berlin, Germany
- Carbone L, Gourc JP, Carrubba P, Pavanello P, Moraci N (2015) Dry friction behaviour of a geosynthetic interface using inclined plane and shaking table tests. *Geotext Geomembr* 43:293–306
- Cardile G, Giofrè D, Moraci N, Calvarano LS (2017a) Modelling interference between the geogrid bearing members under pullout loading conditions. *Geotext Geomembr* 45:169–177
- Cardile G, Moraci N, Calvarano LS (2016a) Geogrid pullout behaviour according to the experimental evaluation of the active length. *Geosynth Int* 23:194–205
- Cardile G, Moraci N, Pisano M (2016b) In-air tensile load-strain behaviour of HDPE geogrids under cyclic loading. *Procedia Eng* 158:266–271
- Cardile G, Moraci N, Pisano M (2017b) Tensile behaviour of an HDPE geogrid under cyclic loading: experimental results and empirical modelling. *Geosynth Int* 24:95–112
- Cardile G, Pisano M, Moraci N (2019) The influence of a cyclic loading history on soil-geogrid interaction under pullout condition. *Geotext. Geomembr.* <https://doi.org/10.1016/j.geotexmem.2019.01.012>
- Dyer MR (1985) Observations of the stress distribution in crushed glass with applications to soil reinforcement. PhD thesis, Magdalene College, University of Oxford, Michaelmas Term, p. 220
- Ezzein FM, Bathurst RJ (2014) A new approach to evaluate soil-geosynthetic interaction using a novel pullout test apparatus and transparent granular soil. *Geotext Geomembr* 42:246–255
- Fannin J, Raju DJ (1993) Large-scale pull-out test results on geosynthetics. In: *Geosynthetics '93*, Vancouver, Canada, pp 633–643
- Ferreira J, Zornberg J (2015) A transparent pullout testing device for 3D evaluation of soil-geogrid interaction. *Geotech Test J* 38:686–707
- Jewell RA (1990) Reinforcement bond capacity. *Geotechnique* 40:513–518
- Jewell RA (1996) *Soil reinforcement with geotextile*. CIRIA Thomas Telford, London
- Matsui T, San KC, Nabeshima Y, Amin UN (1996) Bearing mechanism of steel grid reinforcement in pullout test. In: *International symposium on earth reinforcement*, Fukuoka, Kyushu, Japan, pp 101–105

- Milligan GWE, Earl RF, Bush DI (1990) Observations of photo-elastic pullout tests on geotextiles and geogrids. In: 4th international conference on geotextiles, geomembranes and related products, pp 747–751
- Moraci N, Cardile G (2008) Pullout behaviour of different geosynthetics embedded in granular soils. In: 4th Asian regional conference on geosynthetics, Shanghai, China, pp 146–150
- Moraci N, Cardile G (2009) Influence of cyclic tensile loading on pullout resistance of geogrids embedded in a compacted granular soil. *Geotext Geomembr* 27:475–487
- Moraci N, Cardile G (2012) Deformative behaviour of different geogrids embedded in a granular soil under monotonic and cyclic pullout loads. *Geotext Geomembr* 32:104–110
- Moraci N, Cardile G, Giofrè D, Mandaglio MC, Calvarano LS, Carbone L (2014) Soil geosynthetic interaction: design parameters from experimental and theoretical analysis. *Transp Infrastruct Geotechnol* 1:165–227
- Moraci N, Cardile G, Pisano M (2017) Soil-geosynthetic interface behaviour in the anchorage zone [Comportamento all'interfaccia terre-no-geosintetico nella zona di ancoraggio]. *Rivista italiana di geotecnica* 51:5–25
- Moraci N, Giofrè D (2006) A simple method to evaluate the pullout resistance of extruded geogrids embedded in a compacted granular soil. *Geotext Geomembr* 24:198–199
- Palmeira EM (2009) Soil-geosynthetic interaction: modelling and analysis. *Geotext Geomembr* 27:368–390
- Palmeira EM, Milligan GWE (1989) Scale effects in direct shear tests on sand. In: Proceedings of 12th ICSMFE, Rio, Brazil, pp 739–742
- Pavanello P, Carrubba P, Moraci N (2018a) The determination of interface friction by means of vibrating table tests. *Geotext Geomembr* 46:830–835
- Pavanello P, Carrubba P, Moraci N (2018b) Dynamic friction and the seismic performance of geosynthetic interfaces. *Geotext Geomembr* 46:715–725
- Raju DM (1995) Monotonic and cyclic pullout resistance of geosynthetic. PhD thesis, University of British Columbia, Vancouver, Canada
- Zhou J, Chen J-F, Xue J-F, Wang J-Q (2012) Micro-mechanism of the interaction between sand and geogrid transverse ribs. *Geosynth Int* 19:426–437